

## Electron-Hole Symmetry and Magnetic Coupling in Antiferromagnetic LaOFeAs

Z. P. Yin<sup>1</sup>, S. Lebègue<sup>1,2</sup>, M. J. Han<sup>1</sup>, B. Neal<sup>1</sup>, S. Y. Savrasov<sup>1</sup>, and W. E. Pickett<sup>1</sup>

<sup>1</sup>*Department of Physics, University of California Davis, Davis, CA 95616 and*

<sup>2</sup>*Laboratoire de Cristallographie et de Modélisation des Matériaux Minéraux et Biologiques,  
UMR 7036, CNRS-Université Henri Poincaré,*

*B.P. 239, F-54506 Vandoeuvre-lès-Nancy, France*

(Dated: June 30, 2021)

When either electron or hole doped at concentrations  $x \sim 0.1$ , the LaOFeAs family displays remarkably high temperature superconductivity with  $T_c$  up to 55 K. In the most energetically stable  $\vec{Q}_M = (\pi, \pi)$  antiferromagnetic (AFM) phase comprised of tetragonal-symmetry breaking alternating chains of aligned spins, there is a deep pseudogap in the Fe 3d states centered at the Fermi energy, and very strong magnetophonon coupling is uncovered. Doping (of either sign) beyond  $x \sim 0.1$  results in Fe 3d heavy mass carriers ( $m^* \sim 4 - 8$ ) with a large Fermi surface. Calculated Fe-Fe transverse exchange couplings  $J_{ij}(R)$  reveal that exchange coupling is strongly dependent on the AFM symmetry and Fe-As distance.

Since the appearance of copper oxide high temperature superconductors (HTS) two decades ago,<sup>1</sup> there has been a determined but underfunded effort to discover related superconductors in two-dimensional (2D) transition metal oxides (TMO), borides, nitrides, etc. Promising developments in this area include  $\text{Li}_x\text{NbO}_2$ ,<sup>[2]</sup>,  $\text{Sr}_2\text{RuO}_4$ ,<sup>[3]</sup>  $\text{Na}_x\text{CoO}_2$ ,<sup>[4]</sup> and  $\text{Cu}_x\text{TiSe}_2$ ,<sup>[5]</sup> but all have superconducting critical temperature  $T_c$  of 5K or less. The most striking discovery was that of electron-doped hafnium nitride semiconductor (HfNC1) [6] with  $T_c = 25$  K. The other distinctive breakthrough,<sup>7</sup>  $\text{MgB}_2$  ( $T_c=40$  K), has strong 2D features but contains only  $s, p$  elements. Recently, design of possible TMO superconductors has been stimulated by a specific approach outlined by Chaloupka and Khalullin.<sup>8</sup>

The simmering state of superconductor discovery has been re-ignited by discovery of a new class of layered transition metal pnictides  $\mathcal{R}\mathcal{O}\mathcal{T}\mathcal{P}\mathcal{n}$ , where  $\mathcal{R}$  is a trivalent rare earth ion,  $\mathcal{T}$  is a late transition metal ion, and  $\mathcal{P}\mathcal{n}$  is a pnictogen atom. The breakthrough of  $T_c=26$  K ( $T_c^{\text{onset}}=32$  K) was reported<sup>9</sup> for  $0.04 \leq x \leq 0.12$  electron doped  $\text{LaO}_{1-x}\text{F}_x\text{FeAs}$ , followed by the demonstration that hole-doping<sup>10</sup> in  $\text{La}_{1-x}\text{Sr}_x\text{OFeAs}$ ,  $0.09 \leq x \leq 0.20$ , leads to a similar value of  $T_c$ . These values of  $T_c$  have now been superseded by the finding that replacement of La by Ce,<sup>11</sup> Pr,<sup>12</sup> Nd,<sup>13</sup> Sm,<sup>14,15</sup> and Gd<sup>16</sup> result in  $T_c = 41-55$  K, substantially higher than in any materials except for the cuprate HTS.

The transport, magnetic, and superconducting properties of  $\text{LaO}_{1-x}\text{F}_x\text{FeAs}$  depend strongly on doping.<sup>9,10,17</sup> Most interestingly, a kink is observed<sup>11</sup> in the resistivity of the stoichiometric (“undoped”

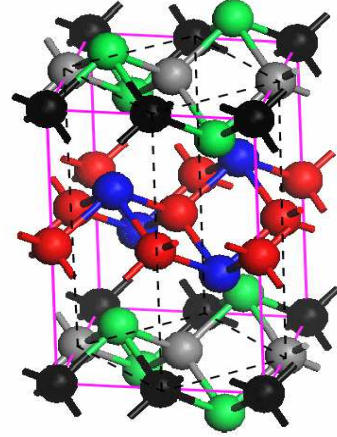


FIG. 1: (color online) The  $Q_M$  antiferromagnetic structure of LaOFeAs, with different shades of Fe atoms (top and bottom planes) denoting the opposing directions of spins in the  $Q_M$  AFM phase. Fe atoms lie on a square sublattice coordinated tetrahedrally by As atoms, separated by LaO layers (center of figure) of similar structure. The dashed lines indicate the nonmagnetic primitive cell.

but conducting) compound, which has been identified with the onset of antiferromagnetism (AFM). As a result, the original focus on the nonmagnetic LaOFeAs compound switched to an AFM ground state, in which the two Fe atoms in the primitive cell have oppositely oriented moments. Due to the structure of the FeAs layer, shown in Fig. 1, that requires two Fe atoms in the primitive cell, this ordering represents a  $Q=0$  AFM state.

The basic electronic structure of this class of compounds was presented for LaOFeP, superconducting

at 5 K [18], by Lebègue.<sup>19</sup> The electronic structure of paramagnetic LaOFeAs is similar, and its (actual or incipient) magnetic instabilities have been described by Singh and Du,<sup>20</sup> who found that the Fermi level ( $E_F$ ) lies on the edge of a peak in the density of states (DOS), making the electronic structure strongly electron-hole *asymmetric*. The Fermi surfaces are dominated by zone center and zone corner cylinders, which underlie several models of both magnetic<sup>21</sup> and superconducting<sup>22,23,24,25</sup> properties. Cao *et al.*<sup>26</sup> and Ma and Lu<sup>27</sup> demonstrated that a  $Q=0$  AFM state (mentioned above) is energetically favored, but coincidentally (because the electronic structure is substantially different) still leaves  $E_F$  on the edge of a DOS peak, *i.e.* strongly particle-hole asymmetric. In both paramagnetic and  $Q=0$  AFM states a degenerate  $d_{xz}, d_{yz}$  pair of Fe orbitals remains roughly half-filled, suggesting possible spontaneous symmetry breaking to eliminate the degeneracy.<sup>21,28</sup> Such degeneracies have attracted attention in transition metal oxides.<sup>29</sup>

Subsequently it was reported by Dong *et al.*<sup>30</sup> that a  $\vec{Q}_M = (\pi, \pi, 0) \sqrt{2} \times \sqrt{2}$  AFM state lies substantially lower still in energy. The spin arrangement consists of Fe chains of aligned spins along one direction (which we take to be the  $x$ -axis) of the square Fe sublattice, with alternate chains having opposite spin direction. This  $\vec{Q}_M$  ordering is what might be expected from the (approximate) nesting of Fermi surfaces in the primitive cell, but the calculated moments are large ( $1.72 \mu_B$  in the  $Q=0$  phase,  $1.87 \mu_B$  for  $Q_M$ ) and thus is far removed from a ‘spin density wave’ description. Neutron scattering<sup>31,32</sup> and x-ray scattering<sup>32</sup> have confirmed this in-plane ordering, and reveal that alternating planes of Fe spins are antialigned, *i.e.* the true ordering is  $(\pi, \pi, \pi)$ .

To prepare for studying the superconducting state, it is necessary first to understand the normal state from which it emerges. Here we analyze the conducting  $Q_M$  AFM phase, using results from two all-electron, full potential codes Wien2k<sup>33</sup> and FPLO<sup>34,35</sup> using the generalized gradient approximation<sup>36</sup> (GGA) functional. We find the  $Q_M$  phase to be energetically favored over the  $Q=0$  AFM phase by  $\sim 75$  meV/Fe, which itself lies 87 meV/Fe below the nonmagnetic phase. This energy difference is large enough that neither the  $Q=0$  AFM, nor the nonmagnetic, phase will be thermally accessible at temperatures of interest. We neglect the antialignment of spins on the well separated adjacent FeAs layers, which will have little effect on the electronic and magnetic structure of a layer due to the weak interlayer hopping. In either AFM phase,

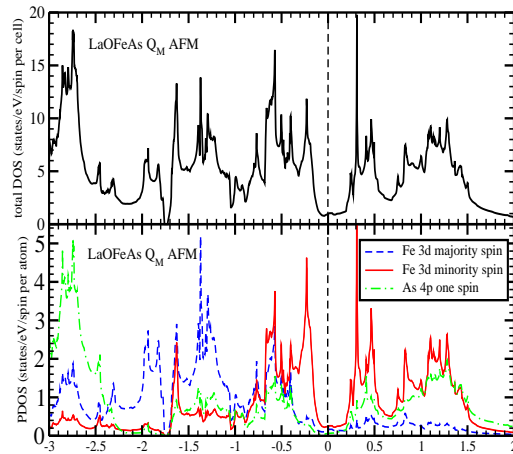


FIG. 2: (color online) Top panel: total DOS for the  $Q_M$  AFM phase. Bottom panel: spin resolved Fe 3d DOS, showing majority filled and minority half-filled up to the pseudogap, and the As 4p DOS.

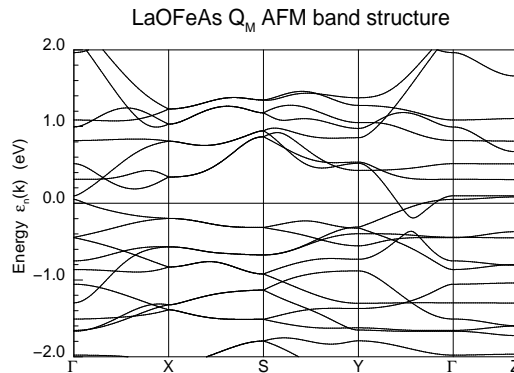


FIG. 3: Band structure of the  $\vec{Q}_M$  AFM phase along high symmetry directions. Note that two dispersive bands and one narrow band cross  $E_F$  along  $\Gamma$ -Y, while only the one flatter band crosses  $E_F$  (very near  $k=0$ ) along  $\Gamma$ -X.

the Fe majority states are completely filled, thus the moment is determined by the occupation of the minority states. From the projected Fe 3d density of states (DOS) shown in Fig. 2, the minority states are almost exactly half-filled, giving 7.5 3d electrons and thus an Fe state that is no more than  $0.5e$  from neutral. While the center of gravity of As 4p weight lies below that of Fe 3p bands, there is strong mixing of these two characters on both sides of  $E_F$ , and the As 4p states are certainly unfilled.

Notably, the band structure and DOS is character-

ized by a pseudogap straddling  $E_F$ , closing only in a small region along the  $\Gamma$ -Y line near  $\Gamma$ . Since the moments, and hence the exchange energies, of the two AFM phases are very similar, the energy gain in the  $Q_M$  phase can be ascribed to the formation of the pseudogap. The system could be considered as *metallic* rather than semimetallic, in the sense that there are two dispersive bands crossing  $E_F$  along  $\Gamma$ -Y. One is 1.3 eV wide, comprised of Fe  $d_{xy}$  + As  $p_z$  character, the other of  $d_{yz}$  character is 0.9 eV wide. A third narrower (0.4 eV) band of  $3d_{x^2-y^2}$  character crosses  $E_F$  near  $\Gamma$ . The crossing of the dispersive bands along  $\Gamma$ -Y are such as to leave only two small distinct 2D Fermi surfaces, shown in Fig. 4: an elliptical hole cylinder at  $\Gamma$  containing  $\sim 0.03$  holes, and two symmetrically placed near-circular electron tubes midway along the  $\Gamma$ -Y axis. In the sense that the Fermi surfaces are small, the state is semimetallic. The bands near  $E_F$  have  $k_z$  dispersion of no more than 25 meV.

The  $d_{xz}, d_{yz}$  degeneracy is broken by the chains of aligned Fe spins in the  $Q_M$  phase. The rough characterization for the minority Fe orbitals is that  $d_{z^2}$  and  $d_{x^2-y^2}$  states are partially filled,  $d_{xy}$  and  $d_{xz}$  states are empty, the  $d_{yz}$  states are mostly filled but giving rise to the hole Fermi surfaces. (Note that here the  $x-y$  coordinate system is rotated by  $45^\circ$  from that usually used for the primitive cell, see Fig. 1.)

A strikingly feature, crucial for accounting for observations, is that the DOS is (roughly) particle-hole symmetric, as is the observed superconducting behavior. All bands near  $E_F$  are essentially 2D, resulting in only slightly smeared 2D-like DOS discontinuities at the band edges with structure elsewhere due to band crossings and non-parabolic regions of the bands. The DOS has roughly a constant value of 0.25 states/(eV Fe spin) within 0.15-0.2 eV of  $E_F$ , with much flatter bands beyond. The hole and electron effective in-plane masses, obtained from  $N(E) = m^*/(\pi\hbar^2)$  for each pocket, are  $m_h^* = 0.33, m_e^* = 0.25$ . An analogous band structure occurs in electron-doped HfNiCl<sub>3</sub>,<sup>37</sup> but there superconductivity appears before the heavy bands are occupied.

There are somewhat conflicting indications of the possible importance of electron-phonon coupling in this compound.<sup>38,39</sup> Fig. 5 provides evidence of strong *magnetophonon* coupling: increase of the As height which changes the Fe-As distance affects the Fe moment at a rate of  $6.8 \mu_B/\text{\AA}$ , indicating an unusually large sensitivity to the Fe-As separation. Fig. 5 also reveals another important aspect: LDA

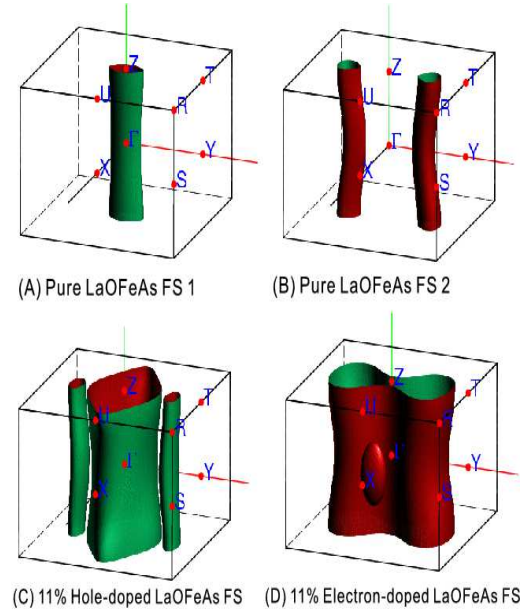


FIG. 4: (color online) Fermi surfaces of LaOFeAs. (A) and (B): the hole cylinders and electron tubes of the stoichiometric  $Q_M$  phase. (C) and (D): hole- and electron-doped surfaces.

and GGA are almost 0.1  $\text{\AA}$  off in predicting the height of the As layer relative to Fe, a discrepancy that is uncomfortable large. Neglecting the Fe magnetism increases the discrepancy.

“Doping” (change of charge in the FeAs layers) is observed to cause the Néel temperature to decrease, and no magnetic order is apparent in superconducting samples. The effect of (rigid band or virtual crystal) doping on the  $Q_M$  electronic structure, either by electrons or holes, is to move  $E_F$  into a region of heavier carriers, by roughly a factor of 20 ( $m_h^* \sim 6 \sim m_e^*$ ). About 0.1 carriers is sufficient to do this, which is just the amount of doping that results in superconductivity. The Fermi surfaces evolve accordingly as shown in Fig. 4: for electron doping the hole cylinder disappears, the electron tubes enlarge and merge; for hole doping the electron tubes decrease in size as the hole cylinder grows and distorts into a diamond-shaped cross section.

The spectrum of magnetic fluctuations is an important property of any AFM phase, and may bear strongly on the emergence of superconductivity. We have calculated from linear response theory the exchange couplings  $J_{ij}(q)$  for all pairs  $\{i,j\}$  within the unit cell, and by Fourier transform the real space exchange couplings  $J_{ij}(R)$ , for the transverse spin-

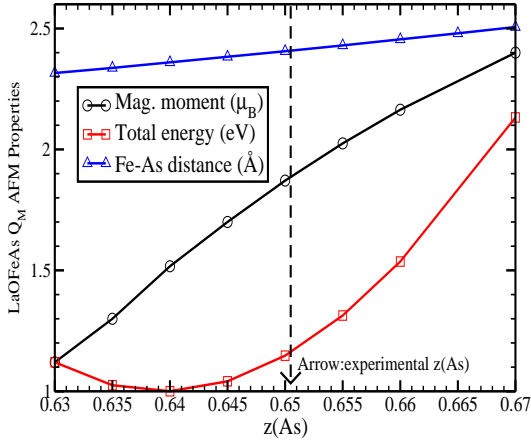


FIG. 5: (color online) The magnitude of the Fe magnetic moment, the change in energy, and the Fe-As distance, as the As height  $z_{As}$  is varied.

wave Hamiltonian<sup>40,41</sup>

$$H = - \sum_{\langle i,j \rangle} J_{ij} \hat{e}_i \cdot \hat{e}_j; \quad J_{ij}(R) = - \frac{d^2 E[\{\theta\}]}{\partial \theta_i(0) \partial \theta_j(R)}, \quad (1)$$

where  $\theta_j(R)$  is the angle of the moment (with direction  $\hat{e}_j$ ) of the  $j$ -th spin in the unit cell at  $R$ . For the  $Q_M$  AFM phase and experimental structural parameters, the 1st and 2nd neighbor couplings are (distinguishing parallel and perpendicular spins)

$$J_1^\perp = -550 \text{ K}; J_1^\parallel = +80 \text{ K}; J_2^\perp = -260 \text{ K}. \quad (2)$$

For comparison, the nearest neighbor coupling<sup>40,41</sup> in elemental FM Fe is  $J_1 \approx 1850 \text{ K}$ , *i.e.* 3-4 times as strong. The signs are all supportive of the actual ordering, there is no frustration. The factor-of-7 difference between the two 1st neighbor couplings

reflects the strong asymmetry between the  $x$ - and  $y$ -directions in the  $Q_M$  phase, which is also clear from the bands. The sensitivity to the Fe-As distance is strong: for  $z(As)=0.635$ , where the moment is decreased by 40% (Fig. 5), the couplings change by roughly a factor of two:  $J_1^\perp = -200 \text{ K}$ ,  $J_1^\parallel = +130 \text{ K}$ ,  $J_2^\perp = -140 \text{ K}$ . The interlayer exchange constants will be much smaller and, although important for the (three dimensional) ordering, that coupling should leave the spin-wave spectrum nearly two-dimensional.

We emphasize that these exchange couplings apply only to small rotations of the moment (spin waves). The  $Q=0$  phase couplings are different from those for the  $Q_M$  phase; furthermore, when FM alignment is enforced the magnetism disappears entirely. The magnetic coupling is phase-dependent, largely itinerant, and as mentioned above, it is sensitive to the Fe-As distance.

The electronic and magnetic structure, and the strength of magnetic coupling, in the reference state of the new iron arsenide superconductors has been presented here, and the origin of the electron-hole symmetry of superconductivity has been clarified. The dependence of the Fe moment on the environment, and an unusually strong magnetophonon coupling, raises the possibility that magnetic fluctuations are involved in pairing, but that it is longitudinal fluctuations that are important here.

W.E.P. thanks Y. Tokura and P. B. Allen for discussions on this system. We acknowledge support from NSF Grants DMR-0608283 and DMR-0606498 (S.Y.S.) and from DOE Grant DE-FG03-01ER45876 (W.E.P.). S.L. acknowledges financial support from ANR PNANO Grant ANR-06-NANO-053-02 and ANR Grant ANR-BLAN07-1-186138.

<sup>1</sup> J. G. Bednorz and K. A. Müller, Z. Physik B **64**, 189 (1986).

<sup>2</sup> M. J. Geselbracht *et al.*, Stacy, Nature **345**, 324 (1990).

<sup>3</sup> Y. Maeno *et al.*, Nature **372**, 532 (1994).

<sup>4</sup> K. Takada *et al.*, Nature **422**, 53 (2003).

<sup>5</sup> E. Morosan *et al.*, Nature Phys. **2**, 544 (2006).

<sup>6</sup> S. Yamanaka *et al.*, Nature **392**, 580 (1998).

<sup>7</sup> J. Nagamatsu *et al.*, Nature **410**, 63 (2001).

<sup>8</sup> J. Chaloupka and G. Khaliullin, Phys. Rev. Lett. **100**, 016404 (2008).

<sup>9</sup> Y. Kamihara *et al.*, J. Amer. Chem. Soc. **130**, 3296

(2008).

<sup>10</sup> H.-H. Wen *et al.*, Europhys. Lett. **82**, 17009 (2008).

<sup>11</sup> G. F. Chen *et al.*, arXiv:0803.3790.

<sup>12</sup> Z.-A. Ren *et al.*, arXiv:0803.4283.

<sup>13</sup> Z.-A. Ren *et al.*, arXiv:0803.4234.

<sup>14</sup> X. H. Chen *et al.*, arXiv:0803.3603.

<sup>15</sup> Z.-A. Ren *et al.*, arXiv:0804.2582.

<sup>16</sup> P. Cheng *et al.*, arXiv:0804.0835.

<sup>17</sup> A. S. Sefat *et al.*, arXiv:0803.2528.

<sup>18</sup> T. Watanabe *et al.*, Inorg. Chem. **46**, 7719 (2007).

<sup>19</sup> S. Lebegue, Phys. Rev. B **75**, 035110 (2007).

<sup>20</sup> D. J. Singh and M.-H. Du, arXiv:0803.0429.

- <sup>21</sup> H.-J. Zhang *et al.*, arXiv:0803.4487.  
<sup>22</sup> I. I. Mazin *et al.*, arXiv:0803.2740.  
<sup>23</sup> X. Han *et al.*, arXiv:0803.4346.  
<sup>24</sup> X. Dai *et al.*, arXiv:0803.3982.  
<sup>25</sup> K. Kuroki *et al.*, arXiv:0803.3325.  
<sup>26</sup> C. Cao *et al.*, arXiv:0803.3236.  
<sup>27</sup> F. Ma and Z.-Y. Lu, arXiv:0803.3286.  
<sup>28</sup> T. Li, arXiv:0804.0536.  
<sup>29</sup> Y. Tsujimoto *et al.*, Nature **450**, 1062 (2007).  
<sup>30</sup> J. Dong *et al.*, arXiv:0803.3426.  
<sup>31</sup> C. de la Cruz *et al.*, arXiv:0804.0795.  
<sup>32</sup> M. A. McGuire *et al.*, arXiv: 0804.0796.  
<sup>33</sup> P. Blaha *et al.*, WIEN2k (K. Schwarz, Techn. Univ. Wien, Austria),2001.  
<sup>34</sup> K. Koepernik and H. Eschrig, Phys. Rev. B **59**, 1743 (1999).  
<sup>35</sup> K. Koepernik *et al.*, Phys. Rev. B **55**, 5717 (1997).  
<sup>36</sup> J. P. Perdew and Y. Wang, Phys. Rev. B **45**, 13244 (1992).  
<sup>37</sup> R. Weht *et al.*, Europhys. Lett. **48**, 320 (1999).  
<sup>38</sup> L. Boeri *et al.*, arXiv:0803.2703.  
<sup>39</sup> H. Eschrig, arXiv:0804.0186.  
<sup>40</sup> A. I. Liechtenstein *et al.*, J. Magn. Magn. Mat. **67**, 65 (1987).  
<sup>41</sup> X. Wan *et al.*, Phys. Rev. Lett. **97**, 266403 (2006).